



HAL
open science

Sensitivity study to select the wet deposition scheme in an operational atmospheric transport model

Arnaud Querel, Denis Quelo, Yelva Roustan, Anne Mathieu

► To cite this version:

Arnaud Querel, Denis Quelo, Yelva Roustan, Anne Mathieu. Sensitivity study to select the wet deposition scheme in an operational atmospheric transport model. *Journal of Environmental Radioactivity*, 2021, 237, pp.106712. 10.1016/j.jenvrad.2021.106712 . hal-03553596

HAL Id: hal-03553596

<https://hal.science/hal-03553596>

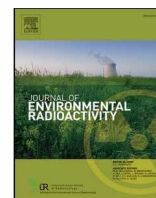
Submitted on 2 Feb 2022

HAL is a multi-disciplinary open access archive for the deposit and dissemination of scientific research documents, whether they are published or not. The documents may come from teaching and research institutions in France or abroad, or from public or private research centers.

L'archive ouverte pluridisciplinaire **HAL**, est destinée au dépôt et à la diffusion de documents scientifiques de niveau recherche, publiés ou non, émanant des établissements d'enseignement et de recherche français ou étrangers, des laboratoires publics ou privés.



Distributed under a Creative Commons Attribution 4.0 International License



Sensitivity study to select the wet deposition scheme in an operational atmospheric transport model

Arnaud Quérel^{a,*}, Denis Quélo^a, Yelva Roustan^b, Anne Mathieu^c

^a IRSN, Institute of Radiation Protection and Nuclear Safety, PSE-SANTE, SESUC, BMCA, Fontenay-aux-Roses, France

^b CEREA, Joint Laboratory École des Ponts ParisTech and EDF R&D, Marne-la-Vallée, France

^c IRSN, Institute of Radiation Protection and Nuclear Safety, PSE-ENV, SEREN, BERAP, Fontenay-aux-Roses, France

ARTICLE INFO

Keywords:

Wet deposition scheme
Fukushima deposit
Atmospheric transport model
Emergency response
Sensitivity study

ABSTRACT

The ability of operational atmospheric transport models to simulate the soil contamination caused by deposition processes is important in the response to a nuclear crisis. The Fukushima accident was characterized by wet deposition of Cs-137, which is difficult to simulate accurately based on observations. A sensitivity study investigated seven wet deposition schemes integrated into operational atmospheric transport models. Deposition maps produced from the multiple simulations are compared with each other and with the observed deposition. Similarities and discrepancies in average behavior are presented for a number of modeling cases on the basis of criteria representing soil contamination crisis management needs. This study confirms the importance of the wet deposition scheme in a crisis management context. None of the schemes used in the study are the best option to satisfy all the comparison criteria. This study suggests that crisis managers must not exclusively trust a single model for selecting responses. At the current time, it is preferable to use several wet deposition schemes in the modelling tools for emergency responses.

1. Introduction

The accidental discharge of large amounts of **radioactive matter** into the environment can affect the health of the population. If the matter is discharged into the atmosphere, the radioactive substances, emitted as gases or particles, are rapidly transported far from the discharge site and partial fallout will occur during transport, leading to radioactive deposits on surfaces (soils, roofs, trees, etc.). When these deposits enter the food chain, they determine the level of long-term exposure faced by populations eating the contaminated food.

Numerical atmospheric transport models can be used to calculate the potential environmental consequences of such an accident. Estimated concentrations of radionuclides in the air and soil deposits can be used to define protective measures for local populations before field observations help to understand the situation. On this basis, emergency response services use forecasts calculated using these models as input to protect the populations from exposure to radiation.

Deposition is a physical process which drives atmospheric gases and particles to the ground either by wet or dry processes. If an atmospheric plume is present during rain, the amount of the total deposit will be approximately equal to that of wet deposit. This complex phenomenon

(Slinn, 1977) comprises several processes, including in-cloud scavenging (incorporation of particles in cloud droplets and removal of those transferred to raindrops), and below-cloud scavenging (scavenging by falling hydrometeors). Many physical values which are complex to obtain are required for the detailed modelling of the overall situation. In fact, one pragmatic approach to operational atmospheric transport models covering spatial resolutions of a few kilometres involves modelling wet deposition in an extremely simplified manner by applying a below-cloud scavenging coefficient and an in-cloud scavenging coefficient. In this study, the *wet deposition scheme* is defined as the combination of these two scavenging coefficients. Today, each operational atmospheric transport model has its own wet deposition scheme, implying a lack of scientific consensus.

The simulated deposits of operational models for the Fukushima accident show discrepancies (Draxler et al., 2015). Even several years after the event, no simulation reproduces the deposition map as measured in a totally satisfactory manner (Kajino et al., 2019; Kitayama et al., 2018; Korsakissok et al., 2013; Morino et al., 2013; Mathieu et al., 2018; Sato et al., 2018, 2020; Science Council of Japan (SCJ), 2014). These difficulties are possibly due to the wet deposition schemes used, but also to other parameters, such as quantities and the dynamics of the

* Corresponding author.

E-mail address: arnaud.querel@irsn.fr (A. Quérel).

<https://doi.org/10.1016/j.jenvrad.2021.106712>

Received 9 February 2021; Received in revised form 31 July 2021; Accepted 1 August 2021

Available online 25 August 2021

0265-931X/© 2021 The Authors. Published by Elsevier Ltd. This is an open access article under the CC BY license (<http://creativecommons.org/licenses/by/4.0/>).

discharge of radioactive substances into the atmosphere, and meteorological data (Nakajima et al., 2017).

The Fukushima accident therefore reminds us that the simulation of wet deposits using atmospheric transport models is still an open research question. Beyond this point, this aspect is still worth considering with respect to responses to future crises and is the core focus of this article. Our research specifically focuses on the role of wet deposition schemes. Is it important to select the appropriate wet deposition scheme in an operational atmospheric transport model? Can an approach centred on this issue applied to the Fukushima accident be used to determine which of the schemes used in operational models is preferable?

To date, no literature study has specifically focused on the wet deposition scheme in operational atmospheric transport models. However, many authors (Arnold et al., 2015; Draxler et al., 2015; Kitayama et al., 2018; Leadbetter et al., 2015; Marzo, 2014; Morino et al., 2011; Quérel et al., 2015; Saito et al., 2015; Sato et al., 2018; Science Council of Japan (SCJ), 2014) took note of the sensitivity of caesium-137 (Cs-137) deposition models when considering the Fukushima accident, but without considering its impact on the management of emergency situations. Arnold et al. (2015) focused on the sensitivity of deposition to meteorological data by studying deposition in an 80 km radius around the nuclear powerplant with two different schemes. Leadbetter et al. (2015) compared five in-cloud scavenging coefficients and five below-cloud scavenging coefficients with precipitation from the numerical weather prediction (NWP) and weather radar measurements in the same scope. Multi-model approaches also exist. Draxler et al. (2015) compared deposits according to different atmospheric transport models and the associated meteorological data. The Science Council of Japan (2014) compared the results of nine atmospheric transport models, each using specific source terms, meteorological data and wet deposition schemes. The sensitivity to wet deposition schemes is not specifically studied in these two studies. Morino et al. (2013) used three wet deposition schemes within a single atmospheric transport model. They showed that the selected scheme had a consequence on estimated caesium-137 deposits. Saito et al. (2015) thus highlight the importance of selecting the in-cloud scavenging coefficient, and the impact of selecting the cloud diagnosis method. Quérel et al. (2015) studied the impact of several wet deposition schemes using simulations incorporating several source terms, dry deposition velocities and rainfall data. This latter study is based on a single source of meteorological data and mainly focused on evaluating the contribution of more complex wet deposition schemes.

The traditional approach to determining parametrisation decisions in a model involves trying several options and identifying which ones give the best results by comparing with observations. We adopted this approach by implementing a wet deposition scheme sensitivity study focusing on caesium-137 deposition after the Fukushima accident. This case study is the most documented one in the nuclear emergency response field, including more than a hundred of hourly gamma dose rate stations (Mathieu et al., 2018) and a hundred of hourly Cs-137 air concentration stations (Oura et al., 2015). These observations are important to validate the timing of each plume passing and deposition.

Our study aims to be exhaustive and cover all parameters playing a role in the simulation of wet deposition. Other components in the modelling chain, in addition to the wet deposition scheme, were integrated in the study framework, including the source term and meteorological data, among other aspects. We decided to approximate user needs in emergency situations for the purpose of the analysis by defining evaluation criteria in relation to crisis management.

This study highlights situations which lead to significant differences when calculating the deposit, exclusively attributable to the change in wet deposition scheme. This confirms why the scheme selected is important, particularly when managing emergency situations. We compared the performances of several schemes in order to determine the best one, in terms of their ability to reproduce the deposition observed for the Fukushima accident. It appears that the best scheme differs

depending on the objectives of the simulation process. Each of the schemes covered in this study are more effective in certain configurations.

When facing a crisis management situation with uncertainties, experts tend to aim to obtain several versions of the same configuration in order to determine the range of potential scenarios. In parallel, the decider must ultimately answer a “yes or no question”, i.e. make a deterministic choice. On this basis, we consider that both a preferred scheme, used to provide an initial emergency response, and several schemes covering the full range of potential responses, are required. We also identified the relative positioning of the responses to the different wet deposition schemes currently used in operational atmospheric transport models.

The second part of this article describes the background required in order to understand the study. The third part describes the sensitivity study implemented and continues, in the fourth part, with a presentation of the deposition evaluation criteria used when managing emergency situations. The fifth and final part gives the results in terms of selecting a wet deposition scheme.

2. Background

This study focuses on the caesium-137 deposited after the Fukushima accident. As this radionuclide is transported in the atmosphere as a particle, this study focuses on the wet deposition of particles (and not gases).

2.1. Description of the wet deposition scheme for atmospheric particles

In this article, a wet deposition scheme is defined as the combination of a below-cloud scavenging coefficient and an in-cloud scavenging coefficient. These two types of particle deposition are considered separately based on the different physical mechanisms at play. For a given rainfall intensity, if aerosols lead to the formation of cloud droplets, in-cloud scavenging will be more efficient than below-cloud scavenging (Flossmann and Wobrock, 2010), and complement particle capture by hydrometeors (rain, snow, etc.). A scavenging coefficient, Λ (in s^{-1}), can be used to quantify the proportion of the activity removed from the atmosphere per unit of time. The change in the atmospheric concentration $c(t)$ (in $Bq\ m^{-3}$) at a given point in time and at a given location is described in atmospheric transport models using the following equation (Makhon'ko, 1967):

$$\frac{dc(t)}{dt} = -\Lambda c(t)$$

No consensus exists in terms of the values of scavenging coefficients and a wide range of values is used in the literature (Duhanyan and Roustan, 2011; Wang et al., 2011; Zhang et al., 2013). Differences representing several orders of magnitude can be observed due to the different approaches used to estimate these coefficients. These coefficients can be taken from *in situ* measurements, obtained directly from theoretical models or quantified experimentally in laboratories. For example, the below-cloud scavenging coefficient can be evaluated *in situ* by measuring the reduction in aerosol concentration during rainfall and assuming that this reduction is solely caused by droplet capture (Chate and Pranesha, 2004; Depuydt, 2013; Laakso et al., 2003; Volken and Schumann, 1993). This assumption ignores other significant effects: incoming horizontal air flow, downdraft (Quérel et al., 2014b), etc. This coefficient can also be determined theoretically (Flossmann and Wobrock, 2010) on the basis of a micro-physical parameter known as collection efficiency, which reflects the fact that particles are captured along the streamlines around rain droplets due to Brownian motion, turbulence and phoretic and electrical forces. This parameter is subject to uncertainty of an order of magnitude as values are frequently based on laboratory experiments, which are complex to both perform and compare (Kerker and Hampl, 1974; Lai et al., 1978; Lemaitre et al.,

2017; Quérel et al., 2014a). The concept of wet deposition schemes was developed to compensate for the difficulty inherent in describing the micro-physical phenomena involved in collection in an atmospheric transport model covering much larger scales in time and space. Wet deposition schemes are ultimately approximations and are not closely related to the physical phenomenon.

In order to apply these schemes, several types of input data are required, however these data may not be available because they are not saved as output from NWP models or they may be over-approximative of the physical aspects of the phenomenon in terms of absolute value or space and time resolutions. In atmospheric transport models, the scavenging coefficient can be parametrised based on the type of suspended matter, for instance, the size distribution of atmospheric particles. The vertical position of the cloud is used to define the volumes within which the in-cloud and below-cloud scavenging coefficients are applied. Finally, precipitation at ground level allows to identify the location of the wet deposit. In general, precipitation can be described more or less precisely using several parameters: intensity on the ground, vertical distribution in the atmosphere and droplet size distribution. This information is obtained based on meteorological observations (weather radar, rain gauge, etc.), NWP data or a combination of these two options (e.g. precipitation nowcasting).

2.2. Characteristics of operational atmospheric transport models

Operational atmospheric transport models are used to simulate and forecast the changing of emergency situations, such as those arising as part of nuclear crisis management. The deposition map obtained by modelling must allow responders to define where specific levels are exceeded with respect to post-accident management by public authorities or to launch a measuring plan. On this basis, one of the targets is to rapidly and as accurately as possible predict deposition resulting from atmospheric discharges.

The modelling chain is subject to a range of uncertainties, therefore models are expected to avoid any amplification of incorrect input data. A rapid response is also required in a crisis management context. The actual complexity of the processes modelled is deliberately simplified for these two reasons. On this basis, an operational atmospheric transport model must, above all, be reliable and easy to use in order to provide a suitable response for evaluation objectives when required. Relatively simple wet deposition schemes are generally used in order to match this operational context.

An atmospheric transport model runs using input data, which could be initially poorly constrained and consolidated as progress is made with the emergency response like, for instance, the radionuclide emission rate. Differing original estimates can be made available simultaneously depending on the information used. In the same way, several alternatives can be used to describe the meteorological situation as accurately as possible, from different bodies. An operational atmospheric transport model also has the advantage that different sources of input data can be used.

Several actors are generally involved in the response to an emergency situation, and each actor will use their own model(s). If an accident occurs, each actor will simulate the deposit, leading to different results, in principle. Prior awareness of the behaviour of models can be used to determine the response of a responders and agencies with respect to the other governmental bodies and to explain any inconsistencies.

2.3. Case study: caesium-137 deposited after the Fukushima accident

The Fukushima accident involved the accidental discharge of radioactive matter and is still a subject of scientific investigation. Mathieu et al. (2018) reviewed the atmospheric transport of plumes and radionuclide deposits during this accident. The discharges from the Fukushima powerplant led to deposits in Japan, mainly on 12, around

15, around 20 and around March 30, 2011 (Chino et al., 2011; Morino et al., 2011; Tsuruta et al., 2014; Yumimoto et al., 2016). March 31, 2011 is considered as the end date for significant emissions (Terada et al., 2012). The total deposit includes several combined contributions from these discharge periods.

It was also caused by several physical phenomena. The wet process prevails (deposition from rain, drizzle or snow) and represents up to 80 % of the total (Hirose, 2016; Quérel et al., 2015; Tsuruta et al., 2014). Other types of processes are also involved: dry deposition and local deposition by fog (Hososhima and Kaneyasu, 2015; Sanada et al., 2018). Scavenging of radionuclide plumes travelling at high altitudes was also inferred (Quérel et al., 2016; Mathieu et al., 2018).

Caesium-137 was one of the main radionuclides deposited during the Fukushima accident. Cs-137 is easier to measure because it indirectly emits characteristic gamma radiation and its half-life of 30 years allows for measurements several years after the accident. A large area is covered by the deposit, as defined based on the detectability limit (10 kBq m⁻²), representing 24,000 km² of Japanese territory in April 2011 (Champion et al., 2013), and spreading at least 250 km from the Fukushima powerplant. The Japanese Ministry of Education, Culture, Sports, Sciences and Technology has published a map per square km (MEXT, 2011a; 2011b) of the Cs-137 and Cs-134 deposition, mainly based on aerial survey.

3. Sensitivity study for deposits based on the wet deposition scheme

This study is based on 252 simulations combining a common modelling framework and different sets of parameters, which may be either input data (e.g. source term) or parametrisations (e.g. several wet deposition schemes). The aim for each parameter used to model the deposit is not to obtain exhaustive results but to represent a certain diversity of these options. On this basis, the study focuses on the many wet deposition schemes and on the drive to vary all parameters considered as significant. We studied 7 wet deposition schemes in 36 configurations, as described below, after reiterating the common simulation framework.

3.1. Common simulation framework

All of the simulations in this study were run with IdX (Groëll et al., 2014), the long-range operational atmospheric transport model used by IRSN for nuclear atmospheric discharges, included in the IRSN's C3X operational platform. This Eulerian type model is taken from the Polair3D model (Mallet and Sportisse, 2004) under the Polyphemus platform (Mallet et al., 2007; Quélo et al., 2007), which is designed to study regional-scale air quality problems. Radioactive filiation and decay processes have been added. IdX has been validated in various contexts such as: the Chernobyl accident (Quélo et al., 2007), ETEX (Quélo et al., 2007), or during comparisons between operational atmospheric transport models by CTBTO (Eslinger et al., 2016; Maurer et al., 2018). IdX was repeatedly used to simulate the Fukushima accident in Japan (Kitayama et al., 2018; Mathieu et al., 2012; Quérel et al., 2015; Sato et al., 2018, 2020), and also formed the basis for comparisons at the request of the Science Council of Japan (2014). IdX was recently applied to the detection of Ruthenium-106 in Europe and the model agreed with measurements to a satisfactory extent (Saunier et al., 2019).

A calculation domain, a set of input data and physical parametrisation values must be defined for IdX simulations. The parameters used for all of the IdX simulations are summarised in Table 1. They relate to the spatial domain, the time interval, the modelling of turbulent atmospheric diffusion and the modelling of the dry deposit. The source terms comprise a single radionuclide, caesium-137, emitted as mono-dispersed particles. Due to simplifications applied based on operational usages, IdX considers particles with a constant size over time, implicitly taken into account through deposition constants.

The calculation domain covers Honshu island in Japan and part of

Table 1
Common parameters.

Parameter	Value
Radionuclide in question	Caesium-137
Horizontal spatial and time-based resolution	0.03° - 10 min
Vertical spatial resolution	[0, 40, 85, 141, ..., 4761, 5546] m - a total of 16 levels.
Spatial domain and simulation period	231 × 231 grid - [136.95–143.91]°E for longitude - [34.0–40.93]°N for latitude - from 11 to 31 March
Vertical diffusion	Troen et Mahrt (1986) in the atmospheric boundary layer, Louis (1981) above this layer.
Dry deposition	Constant deposition velocity of 2×10^{-3} m s ⁻¹

the nearby sea in order to simulate the plumes discharged towards the Pacific Ocean, which later return over Japanese land (Terasaka et al., 2016). The horizontal resolution of 0.03° (approx. 3 km) ensures that mountains are approximately modelled, as well as orographic meteorological phenomena. Simulations covered the period from 11 to March 31, 2011.

Matter is transported in the atmosphere by advection (calculated using the wind of the NWP data) and by turbulent diffusion. Vertical turbulent diffusion is modelled in the atmospheric boundary layer by the Troen et Mahrt scheme (1986). Outside of this layer, turbulent diffusion is modelled using the scheme of Louis et al. (1981). The decision was reached not to model horizontal turbulent diffusion as this phenomenon is assumed to be covered by the numerical diffusion inherent to modelling advection.

A dry deposition velocity depending on particle size and soil types (Zhang et al., 2001) failed to demonstrate a major impact according to Quérel et al. (2015), therefore a constant value of 2×10^{-3} m s⁻¹ was used in this study.

3.2. Configurations

Excluding the wet deposition scheme (covered in the following section), the source term and meteorological data are the most sensitive parameters for deposition (Girard et al., 2016). Several options were considered for each parameter, as listed in Table 2. Close attention was paid to two meteorological parameters: rainfall and the cloud diagnosis. A total of 36 configurations were obtained by combining three source terms, three sources of meteorological data, two types of rain data and two cloud diagnoses.

The three source terms are taken from an inverse modelling process used to estimate the discharge rates in order to match observations as closely as possible. The source term used by Katata et al. (2015) is one of the most frequently used terms in the literature. This estimation integrates observations of caesium-137 concentrations on the surface of the Pacific Ocean, air concentrations of caesium-137 in Japan and dose rate measurements. Saunier et al. (2013) estimated their source term based on observed dose rates. Saunier et al. (2016) used air concentrations of caesium-137, particularly those of Oura et al. (2015).

Meteorological data were taken from Sekiyama et al. (2017),

Table 2
Variable parameters other than wet deposition schemes.

Parameter	Value
Source term	Katata et al. (2015) Saunier et al. dose rate (2013) Saunier air concentration (2016)
Meteorological data	Sekiyama et al. (2017) – member 1 Sekiyama et al. (2017) – member 2 Sekiyama et al. (2017) – member 8
Precipitation data	From meteorological data Radar RAP (Saito et al., 2015)
Cloud diagnosis	Fixed cloud height (500 m) Cloud where $Q_c > 10^{-5}$ kg kg ⁻¹

completed by a more recent analysis (Sekiyama et al., 2021). These data were simulated using NHM (Non-Hydrostatic Model), the NWP model of the Japan Meteorological Agency (JMA) by implementing a Local Ensemble Transform Kalman filter (LETKF) data assimilation scheme specially programmed for the Fukushima accident. Three members of this ensemble were selected at random: members 1, 2 and 8.

A minimum threshold of 0.1 mm h⁻¹ was applied to NWP rainfall data to eliminate numerical noise (Costa et al., 2010; Stephan et al., 2008). In addition to these rainfall data, weather radar observations (Saito et al., 2015) were used, in a similar manner to Leadbetter (2019). These observations – known as radar RAP – are data measured by a radar system and corrected by the rain gauges in the AMeDAS meteorological metrology system (AMeDAS, 2011). Light rain is sometimes absent as rainfall intensity is below the detection limit of 0.4 mm h⁻¹ in this case.

Cloud heights and bases (altitudes) must be available in order to differentiate between in-cloud and below-cloud scavenging. This information is not generally available directly in NWP data. The default configuration for the IdX model assumes a single and homogeneous altitude, which remains constant over time, defining the vertical area below the cloud and in the cloud. A more realistic cloud diagnosis was also used. This diagnosis estimates the presence of a cloud above a threshold based on cloud water contents (Q_c), which are defined as the ratio between the mass of the liquid water content of a cloud and the air mass for a given volume. Quérel et al. (2017) recommended a threshold Q_c value of 10^5 kg kg⁻¹, which is suitable for the meteorological data used in this study.

3.3. Presentation of the seven selected wet deposition schemes

The wet deposition schemes studied correspond to those used in the atmospheric transport models: MLDP0, FLEXPART, HYSPLIT, NAME and RATM. They were used to model atmospheric deposition from the Fukushima accident as part of the WMO comparison (Draxler et al., 2012, 2015). These schemes were integrated in the IdX atmospheric transport model based on the data available in Draxler et al. (2012). These are in fact imitations, and the scheme could have been modified since this time in these models. In order to avoid any confusion, they are designated as XX_wds , where “wds” means “wet deposition scheme” and “XX” corresponds to the first 2 letters of the model.

This list is completed by two wet deposition schemes used in IdX. Table 3 shows the formulations used to determine the scavenging coefficients for these seven schemes.

The most complex version of below-cloud scavenging coefficients (Λ), are of type $\Lambda = aI^b$, depending on rainfall intensity (I). In-cloud scavenging coefficients use a wider range of formulations and input data. The parametrisation of ML_wds , inspired by Pudykiewicz (1989) depends on relative humidity and leads to scavenging above a relative humidity threshold of 75 %. The FL_wds wet deposition scheme is described in the article by Arnold et al. (2015). In-cloud scavenging corresponds to the original version of the scheme described by Hertel et al. (1995), which considers the in-cloud scavenging coefficient as the ratio between the rainfall water mass and the mass of water in the cloud, which is then corrected by the integration factor for atmospheric particles in the cloud droplets and ice crystals. The wet deposition scheme HY_wds is described in the User guide for 2016 (Draxler et al., 2016), with constant in-cloud and below-cloud scavenging coefficients. The NA_wds wet deposition scheme used here is taken from Leadbetter et al. (2015). The RA_wds wet deposition scheme is formulated as defined by Hertel et al. (1995) in this study, with a local liquid water content obtained directly from meteorological data instead of an estimate based on rainfall intensity at ground level, as was the case in the original scheme.

The IdX wet deposition scheme used previously to simulate the Fukushima accident (Girard et al., 2016; Groëll et al., 2014; Quérel et al., 2015; Saunier et al., 2013, 2016) combines identical in-cloud and below-cloud scavenging coefficients. This scheme is named “ IdX_wdsI ”. This in-cloud scavenging coefficient is low compared with the range of

Table 3
Wet deposition schemes. I is the rain intensity in $\text{mm}\cdot\text{h}^{-1}$.

Atmospheric transport model	Wet deposition scheme	Below-cloud scavenging coefficient	In-cloud scavenging coefficient	Reference
MLDP0 (version 12)	ML_wds	None ($\Lambda = 0$)	$\Lambda = f \times 3 \times 10^{-5}$ with f the cloud fraction defined by Pudykiewicz (1989) with a threshold of 75 %	D'Amours and Malo (2004)
FLEXPART (version 9.3)	FL_wds	$\Lambda = 10^{-4}I^{0.8}$	$\Lambda = \frac{f_{mc}I}{3.6 \times 10^6 \times cl \times H}$ $cl = 2 \times 10^{-7}I^{0.36}$ cl estimated cloud water content f_{mc} mass ratio of particles integrated in the cloud (=0.9) H cloud height	(Arnold et al., 2015; Hertel et al., 1995)
HYSPLIT	HY_wds	$\Lambda = 8 \times 10^{-5}$	$\Lambda = 8 \times 10^{-5}$	Draxler et al. (2016)
NAME	NA_wds	$\Lambda = 8.4 \times 10^{-5}I^{0.79}$	$\Lambda = 3.36 \times 10^{-4}I^{0.79}$	Leadbetter et al. (2015)
RATM	RA_wds	$\Lambda = 2.98 \times 10^{-5}I^{0.75}$	$\Lambda = \frac{0.9 \times I}{LWC \times H}$ with H the cloud height and LWC the liquid water content	MRI (2015)
ldX (2013)	ldX_wds1	$\Lambda = 5 \times 10^{-5}I$	$\Lambda = 5 \times 10^{-5}I$	Groëll et al. (2014)
ldX	ldX_wds2	$\Lambda = 5 \times 10^{-5}I$	$\Lambda = 5 \times 10^{-4}I^{0.64}$	This study

values found in the literature, therefore a second formulation (“ ldX_wds2 ”) was defined for which the coefficient a was multiplied by 10 and coefficient b was defined at a value of 0.64 to match the equivalent coefficient in the original scheme from Hertel et al. (1995).

The scavenging coefficients used in this study are plotted as a function of rainfall intensity in Fig. 1 to illustrate their variation range. These coefficients were calculated using the meteorological data from member 1 on 15 March. With in-cloud scavenging (Fig. 1b), several scavenging coefficients exist for each rainfall intensity since the formulation used in RA_wds , FL_wds and ML_wds include input data other than rainfall intensity.

The below-cloud scavenging coefficients used in this study are within the scheme variation range found in the literature, which runs from 10^{-8} to 10^{-2} s^{-1} (Duhanyan and Roustan, 2011). They vary by a factor of approximately ten, except HY_wds , which is constant. This scheme is substantially different to the other schemes, particularly for low rain levels.

The in-cloud scavenging coefficient is much higher than the below-cloud coefficient for most wet deposition schemes, with the exception of HY_wds and ldX_wds1 . For the same rainfall intensity, the scavenging coefficients of FL_wds can vary by a factor of 10, and by a factor of 100 for RA_wds . ML_wds varies less around its median value, remaining between 10^{-5} and $4 \times 10^{-5} \text{ s}^{-1}$. The in-cloud scavenging coefficients range from 10^{-5} s^{-1} to 0.5 s^{-1} and differences between models can reach four orders of magnitude.

Such differences must be considered based on their use in atmospheric transport models, when they are taken as the power of an exponential function, mitigating the impacts on deposition. Fig. 2 shows

the scavenging ratio after 10 min, based on rainfall intensity for below-cloud (a) and in-cloud (b) scavenging coefficients. This scavenged ratio increases with rainfall intensity, except for HY_wds , where it remains constant. This ratio can vary between a few percent and almost all of the matter in the atmospheric column. At a given rainfall intensity, the final deposits obtained thus vary widely depending on the scavenging coefficient.

Actual emergency situations for atmospheric transport are modelled as plumes, i.e. fields with inhomogeneous concentrations, which displace and occasionally cross paths with precipitation of varying intensity. The situation becomes even more complex when exclusively attempting to compare the effects of wet deposition schemes. Table 4 illustrates the case study by combining the simulated deposits as mean values for the 36 configurations sharing the same wet deposition scheme and indicates the distribution of the different deposition components: in-cloud scavenging, below-cloud scavenging and dry deposition. Results vary to a fairly small extent when compared with the orders of magnitude of the differences between scavenging coefficients.

The deposit simulated by the different wet deposition schemes may vary by twice as much, however the measurement remains within this range ($1.84 \times 10^{15} \text{ Bq}$, MEXT 2011a; 2011b). This correlates with the scavenging efficiencies of the different schemes. The distribution of the different processes has not been measured. On this basis, only distribution differences between schemes can be identified, their pertinence cannot be assessed. FL_wds and RA_wds on the one hand, and ldX_wds2 and NA_wds on the other hand, generated similar mean deposits (around $2.4 \times 10^{15} \text{ Bq}$ and $2.15 \times 10^{15} \text{ Bq}$ respectively). The percentage of the deposit attributable to in-cloud scavenging for RA_wds is mostly

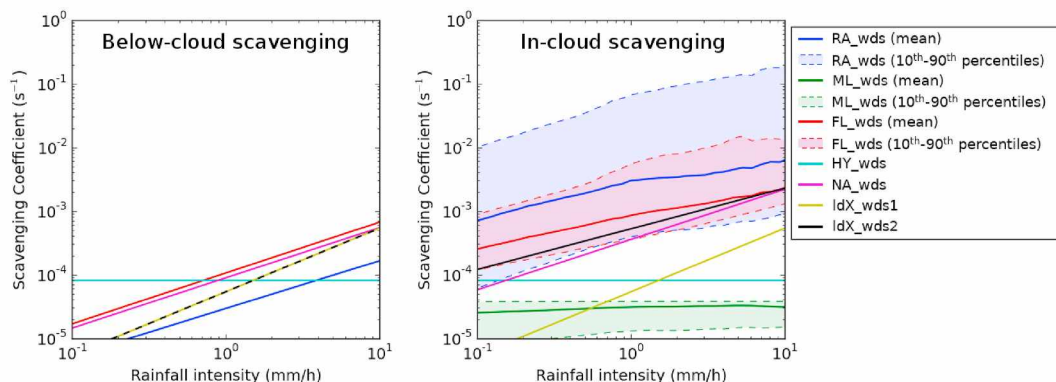


Fig. 1. Scavenging coefficients of the different wet deposition schemes. Solid lines represent the mean on the spatial domain on the March 15, 2011. Dashed lines represent the first and ninth deciles of the scavenging coefficient distributions.

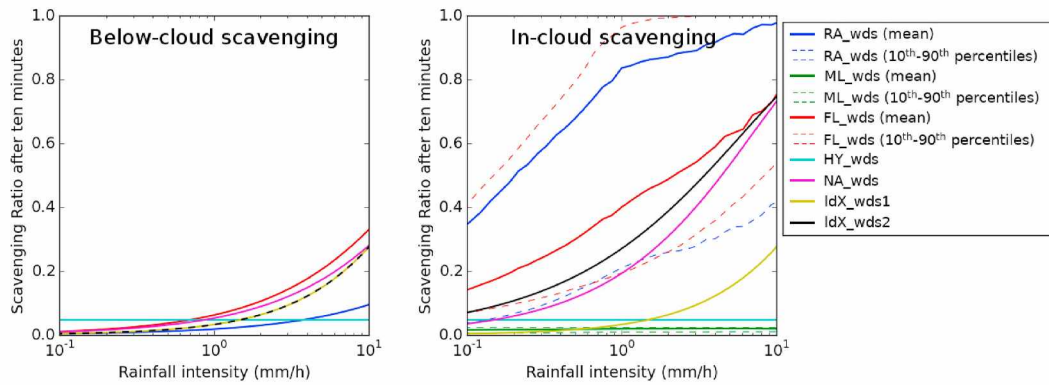


Fig. 2. Scavenging ratio per 10 min of different wet deposition schemes. Solid lines represent the mean on the spatial domain on March 15, 2011. Dashed lines represent the first and ninth deciles of the scavenging coefficient distributions.

Table 4

Deposition in Japan and distribution between the different processes according to the wet deposition scheme. Mean values are shown for all configurations.

Wet deposition scheme	Deposit (x 10 ¹⁵ Bq)	in-cloud	below-cloud	Dry deposition
FL_wds	2.47	49 %	25 %	26 %
RA_wds	2.42	61 %	12 %	27 %
ldX_wds2	2.20	50 %	20 %	30 %
NA_wds	2.13	40 %	30 %	30 %
HY_wds	1.99	24 %	44 %	32 %
ldX_wds1	1.50	20 %	36 %	44 %
ML_wds	1.16	39 %	0 %	61 %

consistent with its higher scavenging efficiency compared with other schemes (cf. Fig. 1). *ldX_wds2* and *NA_wds* make relatively similar contributions. This could be due to the identical formulation of scavenging coefficients based on $\Lambda = aI^b$ with similar constants. *ldX_wds1* and *ML_wds* lead to the smallest deposits. *ldX_wds1* is different due to its lower in-cloud scavenging efficiency and *ML_wds* due to the lack of below-cloud scavenging.

4. Deposit evaluation criteria based on crisis management needs

Decision-makers involved in post-accident nuclear crisis management have three concerns in terms of deposition: where? How much? How? A statistical indicator can be assigned to each of these questions. The indicators used in this study are defined later in this section. They are generally used to evaluate the performances of atmospheric dispersal models. They can be used to rapidly and objectively evaluate the agreement between two deposition maps as part of this process.

Where are the deposits located? One of the first actions required when managing a crisis is to define which areas may be contaminated. The Figure of Merit in Space (FMS) can be used to appraise this criterion by indicating if two surfaces (S_A and S_B) coincide, by calculating the ratio between the intersection and where these surfaces overlap. Perfect agreement will lead to an FMS of 1. In this study, contaminated surfaces are defined by a threshold equal to 10 kBq m⁻² for caesium-137 deposition, which corresponds to the detectability limit for the airborne observations provided by MEXT (2011a, 2011b).

$$FMS = \frac{S_A \cap S_B}{S_A \cup S_B}$$

What quantities are expected? Identifying contamination levels in affected areas helps to prepare for crisis management in these areas. The Factor 2 indicator (FAC2), which determines the proportion of points where values differ by less than a factor of two, was used to aggregate ad hoc deposition evaluations. FAC2 is between 0 and 1 and agreement increases as the value approaches 1.

$$FAC2 = \frac{1}{N_{cell}} N \left(\frac{1}{2} \mu_i^A \leq \mu_i^B \leq 2 \mu_i^A \right)$$

FAC2 was calculated within a surface area with a known total number of grid squares N_{cell} . When comparing a simulation and the observation, the surface with an observed deposit in excess of 10 kBq m⁻² is used. When comparing two simulations, the union of surfaces with a simulated deposit in excess of 10 kBq m⁻² is used. μ_i^A is equal to the surface deposit in grid square i on map A (spatial mean $\bar{\mu}^A$) and μ_i^B is the value of this same grid square on map B (spatial mean $\bar{\mu}^B$).

How is the deposit distributed? Variation in deposition within a given area must also be entered in order to allow crisis operators to plan for likely variations in deposition levels. The Pearson Correlation Coefficient (PCC) was used to model this criterion. This coefficient quantifies the linear relation between two variables, i.e. these variables vary in the same direction and with the same intensity. In this study, the PCC was calculated within the same surface as described for FAC2. The PCC is between -1 and 1 and agreement increases as the value approaches 1.

$$PCC = \frac{\sum_{i=1}^{N_{cell}} (\mu_i^A - \bar{\mu}^A) (\mu_i^B - \bar{\mu}^B)}{\sqrt{\sum_{i=1}^{N_{cell}} (\mu_i^A - \bar{\mu}^A)^2 \sum_{i=1}^{N_{cell}} (\mu_i^B - \bar{\mu}^B)^2}}$$

In practice, the three statistical indicators (FMS, FAC2 and PCC) have been calculated to quantify the differences between the simulated deposition maps (252 simulations of caesium-137 deposits) and the agreement of each of these deposition maps with observations. The indicators are given as percentages throughout the remainder of this study to simplify understanding.

5. Results and discussions

This section presents results over three sections (5.2, 5.3 and 5.4), which relate to the problems mentioned in the introduction: the importance of selecting a wet deposition scheme when managing accident situations, attempting to identify the most effective schemes based on observed deposits after the Fukushima accident and, for the latter, knowledge of their relative responses.

5.1. General scope of the study

Prior to the study of the wet deposition scheme, the general scope of the results of the study was considered. Step one involved checking that the simulated deposits, as a whole, could be used to study the influence of the wet deposition scheme, and particularly check that this input is not masked by a different and more decisive parameter. The second step involved checking that no systematic error occurred when comparing with observations, which would annul the efficiency of the deposition

schemes. Although modelling of the Fukushima accident is known to be incomplete (Nakajima et al., 2017), the schemes generally applied in conditions such as the radionuclide plume must still be correctly combined with rainfall.

This paragraph focuses on the type of deposits simulated as a whole. These deposits are taken as a statistical sample within a parametric space. Are the deposits distributed in a continuous and homogeneous manner? At what point do the simulated deposits diverge? A scatterplot of the simulations is presented in Fig. 3. Each point on the scatterplot corresponds to a simulated deposition result and the colour changes in the 4 sub-figures depending on which parameter is highlighted. The distance between two points is inversely proportional to the PCC of their deposits. On this basis, two points are similar if the deposits represented strongly correlate. This scatterplot is centred with few clusters and each parameter gives a plume distribution. Only the source term shows 3 clusters of points. On this basis, the parametric space covered by this study corresponds to a single block with a homogeneous distribution. The most influential variable is the source term, however this variable cannot systematically explain the PCC between two simulated deposits. The same process was applied to the FMS and FAC2 (not shown here) and led to similar conclusions. The influence of the wet deposition scheme can therefore be studied in this framework.

In order to ensure that the wet deposition schemes were applied in satisfactory conditions, scores reflecting agreement with observations were compared with previous publications using values for the same statistical indicators used in this study. Table 5 shows the minimum and maximum values of these indicators taken from five similar studies.

The deposits simulated in this study moderately agree with observations: FMS vary between 29 and 48 %, FAC2 between 16 and 44 % and PCC between 26 and 59 %. The differences between minimum and maximum indicators are relatively minor, reflecting homogeneous performances for all simulations. The ranges of values obtained are globally smaller than that of other studies, with lower maximum values. A possible explanation is the use of a very positive configuration where the source term was reconstructed to match the observed deposits. Another possible explanation is the use of a less positive configuration where the source term was not reconstructed to match the observed deposits. We selected source terms unaffected by either observed deposits or meteorological data for our study, to avoid any unrealistic bias when applying the deposition schemes.

These rather low indicators could mean that none of the schemes tested are sufficiently representative of the scavenging processes. However, we consider that modelling errors for the other simulation components for the Fukushima accident (meteorological data and the source term in particular) led to many incorrectly modelled episodes for which the attempts to obtain correct results by applying better wet deposition schemes were fruitless. To give one example, meteorological modelling errors are known to be significant in Nakadori valley (Mathieu et al., 2018) – home to the town of Koriyama, 61 km to the east of the Fukushima powerplant. This town is located in a region where deposition is difficult to model due to the air trapped in the valley,

Table 5

Minimum and maximum values of the statistical indicators taken from several studies.

Study		FMS	FAC2	PCC
[min–max] values	This study	[29 %–48 %]	[16 %–44 %]	[26 %–59 %]
	Quérel et al. (2015)	[0 %–59 %]	[0 %–60 %]	[34 %–92 %]
	Katata et al. (2015)	–	[39 %–43 %]	[41 %–67 %]
	Morino et al. (2013)	–	[35 %–57 %]	[31 %–72 %]
	SCJ model intercomparison (Science Council of Japan (SCJ), 2014)	[26 %–74 %]	[14 %–57 %]	[27 %–85 %]
(Sato et al., 2018)*	[39 %–63 %]	–	[50 %–64 %]	
*Only models using met. data, Sekiyama et al. (2017)				

complex wind directions and low rainfall. In this location, the deposition occurred in the form of wet deposits and they were measured on March 15, 2011 between 04:00 and 06:00 UTC (Saunier et al., 2013), which is not the case for all of the simulations run in the study. To understand this point, variation over time on this date was extracted at this location and can be seen in Fig. 4 for air concentration at ground level, rainfall and deposits.

Fig. 4 (a) shows the air concentrations and indicates that the model simulates the passing of a plume at various times, all before 05:00. Fig. 4 (b) shows the different rainfall data. None of these figures shows rainfall between 04:00 and 06:00. Fig. 4 (c) shows variation over time for simulated deposits (shown in green) and the final deposits measured after the event (dashed red line) (MEXT, 2011a; 2011b). The earliest deposit starts at 06:00, however the main deposits formed either at 08:00 or between 14:00 and 18:00, caused by the simultaneous presence of the plume and rainfall. On this basis, no simulation can reproduce the conditions of the observed deposits, between 04:00 and 06:00 UTC, at Koriyama. While two simulations indicated deposition with less than 5 kBq.m⁻² in discrepancy from observations, they focused on the incorrect time span, in conditions where the plume passage and rainfall do not match the actual situation, in principle.

The wet deposition schemes are sometimes applied in modelling conditions which do not accurately represent the conditions at the time. On this basis, it appears preferable to consider the results of this study comparing modelling with observations with caution (section 5.3). The other results (sections 5.2 and 5.4) can be considered as general in scope.

5.2. The importance of selecting a wet deposition scheme when evaluating the consequences of accidents

This section considers the impact of changing wet deposition scheme on how emergency situations are managed based on deposition data. The importance of this aspect was highlighted by focusing on the maximum potential differences obtained for the deposits simply by

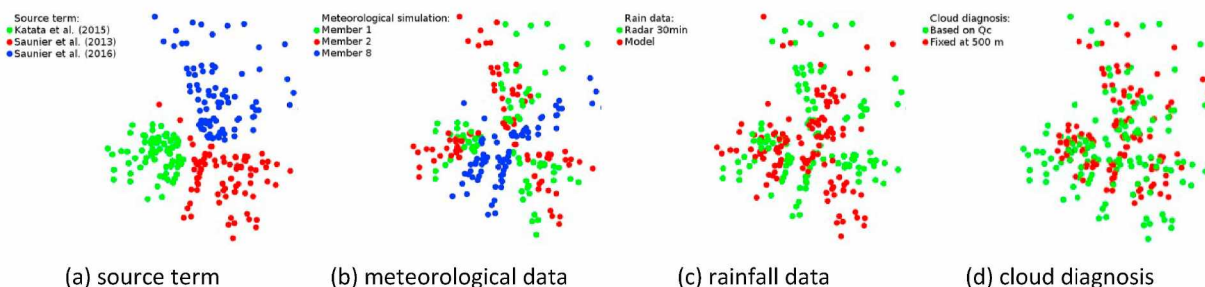


Fig. 3. Scatterplot representing deposits from all simulations – the distance between two points corresponds to the degree of correlation (PCC). The colour depends on the selected parameter. (For interpretation of the references to colour in this figure legend, the reader is referred to the Web version of this article.)

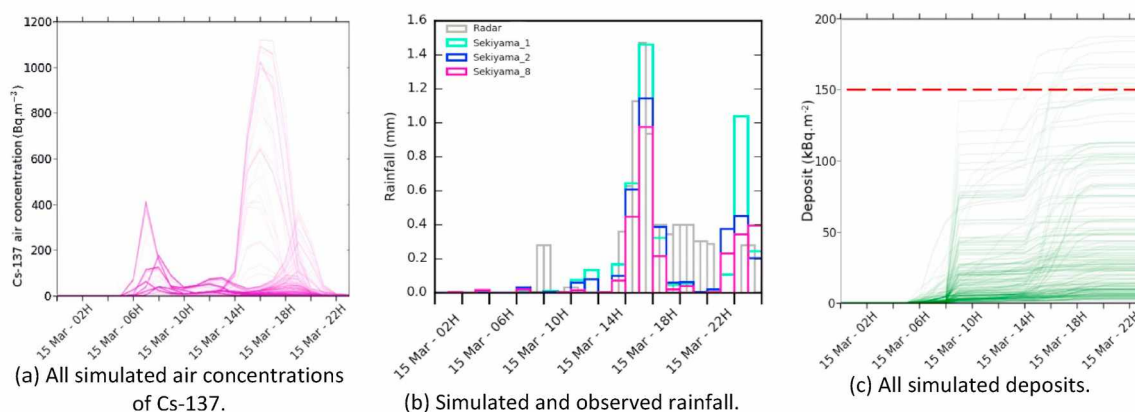


Fig. 4. Variation over time for this study's simulations at Koriyama for (a) Cs-137 air concentration at ground level; (b) rainfall data; (c) Cs-137 deposits. The dashed red line indicates observed deposits. Time in UTC. (For interpretation of the references to colour in this figure legend, the reader is referred to the Web version of this article.)

changing this scheme. The quantification and type of differences obtained in this way were examined using the statistical indicators described in 4.

Three configurations (one for each statistical indicator) were selected to illustrate the impact of the wet deposition scheme. These configurations are described in Table 6 with the source term, meteorological data, rainfall and cloud diagnosis indicated. A pair of wet deposition schemes is selected and listed in the table for each configuration. The statistical indicator is used to quantify differences between the deposition maps resulting from each wet deposition scheme of the pair. The value of the selected pair is indicated in row 2 and the minimum value over all the possible configurations is given between brackets.

Configuration 1 gives the lowest FMS (53 %) out of all of the simulations. This configuration involves the deposit surface areas obtained using *ML_wds* and *FL_wds*. The respective maps can be viewed in Fig. 5 — maps (a) and (b). If the central part of the deposit covers similar surfaces, *FL_wds* leads to deposits to the north of the discharge site, unlike *ML_wds*. On the other hand, *ML_wds* is the only scheme to generate a deposit over a large surface area to the south west. In order to more clearly highlight agreements and discrepancies, three coloured areas are added to Fig. 5 (c): blue = the surface area only simulated using *ML_wds*, red = the surface area only simulated using *FL_wds* and magenta = the surface area simulated using both schemes. The different deposits identified for the two schemes are attributable to the different formulations used, as *ML_wds* excludes wet below-cloud deposition. On this basis, if the plume is located under the cloud, the simulation with *FL_wds* generates a wet deposit in case of rain, whereas no such deposit occurs with *ML_wds*.

In configuration 2, the deposition maps obtained using *ML_wds* and

Table 6

Configurations used to illustrate the impact of selecting a wet deposition scheme.

Configuration number	1 - To illustrate FMS	2 - To illustrate FAC2	3 - To illustrate PCC
Statistical indicator	FMS 53 % (min. 53 %)	FAC2 24 % (min. 17 %)	PCC 82 % (min. 82 %)
Source term	Saunier et al. (2016)	Katata et al. (2015)	Saunier et al. (2013)
Met. Data	8th member of Sekiyama et al. (2017) ensemble	2nd member of Sekiyama et al. (2017) ensemble	2nd member of Sekiyama et al. (2017) ensemble
Rain data	Radar RAP	Model	Model
Cloud diagnosis	Based on cloud water mixing ratio	Based on cloud water mixing ratio	Based on cloud water mixing ratio
Wet deposition schemes	<i>ML_wds</i> <i>FL_wds</i>	<i>ML_wds</i> <i>NA_wds</i>	<i>RA_wds</i> <i>ldX_wds1</i>

NA_wds were shown in Fig. 6 - maps (a) and (b). The deposit simulated by *ML_wds* is less widespread than that simulated using *NA_wds*, however no systematic bias is observed: areas with thicker deposits under one of the schemes and vice versa. The ratio between the two deposition maps is shown in Fig. 6 (c) in order to highlight this aspect. The surface area where the two schemes give equal deposition give or take a factor of 2 (shown in green on the map) represents 24 % of the coloured areas. The surface areas where one of the two simulations overestimates the other by more than a factor of 2, and vice versa, (shown in orange and red) represents the rest of the map.

In configuration 3, the two deposition maps were obtained using the wet deposition schemes *RA_wds* and *ldX_wds1* — maps (a) and (b) in Fig. 7. The grainy appearance of these deposits is more significant when simulated using *RA_wds* rather than *ldX_wds1*. This aspect is quantified by a 82 % correlation (PCC). Fig. 7c complements these data and shows a particularly dispersed scatterplot for deposits for all values.

To summarise, for the three configurations highlighted, simply changing the wet deposition scheme in one simulation has a significant impact on the deposition map, which is likely to affect crisis management by modifying contaminated surfaces and deposition levels. The importance of selecting this scheme is thus underscored.

This sensitivity to the selected scheme varies across the simulations: from 53 to 95 % for FMS, from 17 to 95 % for Factor 2 (FAC2) and from 82 to 99 % for correlation (PCC). This demonstrates that changing scheme will not systematically have the same effect depending on the configuration parameters. To illustrate this point, deposition surfaces in excess of 10 kBq m⁻² obtained using the seven schemes were superposed for two configurations (Fig. 8), those leading to the minimum and maximum envelope FMS out of the 7 schemes. All aspects of these configurations are different, particularly rain data, which are taken from two different meteorological models (see legend). The yellow areas on the maps identify the overlapping surface of the deposits simulated using the seven schemes, while the magenta colour identifies the surface areas where only a single scheme gives a deposit in excess of 10 kBq m⁻². On map (a), the surface area with seven overlapping schemes (yellow) is relatively small for the others compared with map (b) particularly in the area to the north of the discharge point. The map configuration (a) therefore shows the full influence of selecting a wet deposition scheme. On the other hand, for map (b), the contaminated surface is approximately similar for all of the wet deposition schemes.

Although the scavenging efficiencies of deposition schemes vary from one extreme to the other (cf. Fig. 2), this is not the case for deposits, which are all rather similar in some configurations and vary in other configurations. An attempt was made to identify common points for configurations which are sensitive to the selected wet deposition scheme, however this process was unsuccessful. When taken

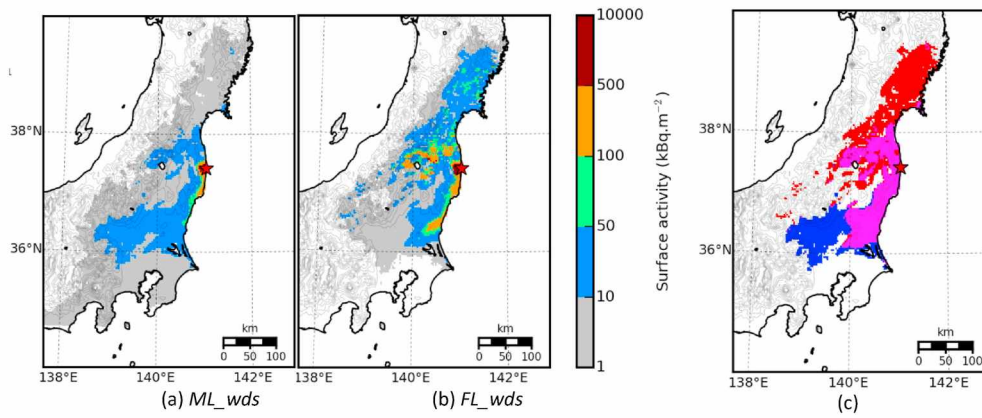


Fig. 5. Deposition maps (kBq m^{-2}) obtained using wet deposition schemes *ML_wds* (a) and *FL_wds* (b) for configuration 1 (see Table 6). (c) Coverage of deposition surfaces above 10 kBq m^{-2} .

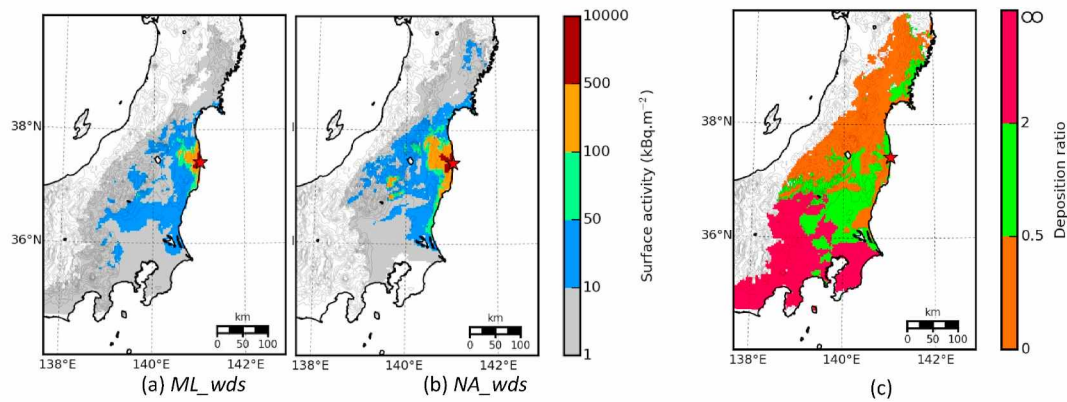


Fig. 6. Deposition maps (kBq m^{-2}) obtained using *ML_wds* (a) and *NA_wds* (b) for configuration 2 (see Table 6). (c) The ratio between these deposition maps.

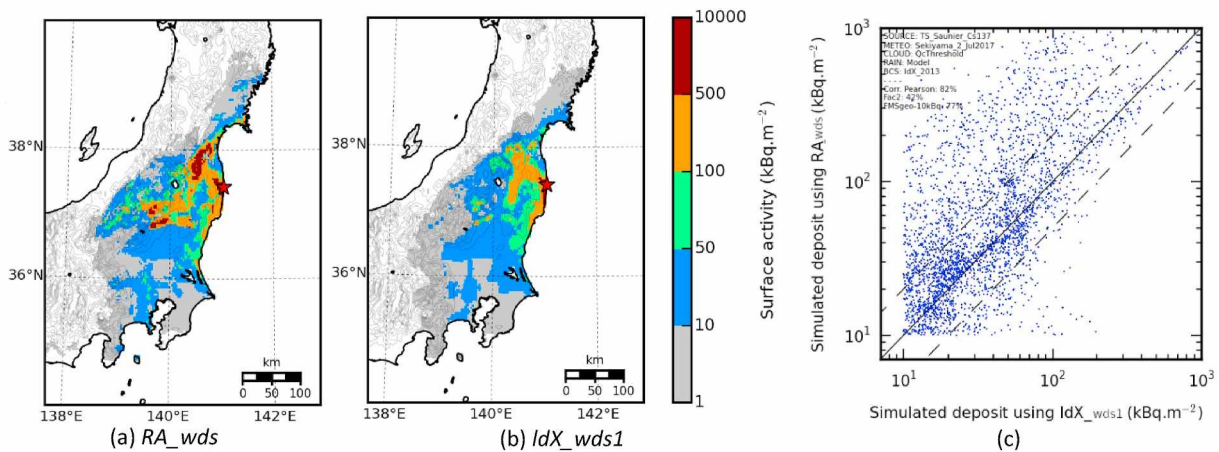


Fig. 7. Deposition maps (kBq m^{-2}) obtained using wet deposition schemes *RA_wds* (a) and *IdX_wds1* (b) for configuration 3 (see Table 6). (c) Scatterplot for these deposits.

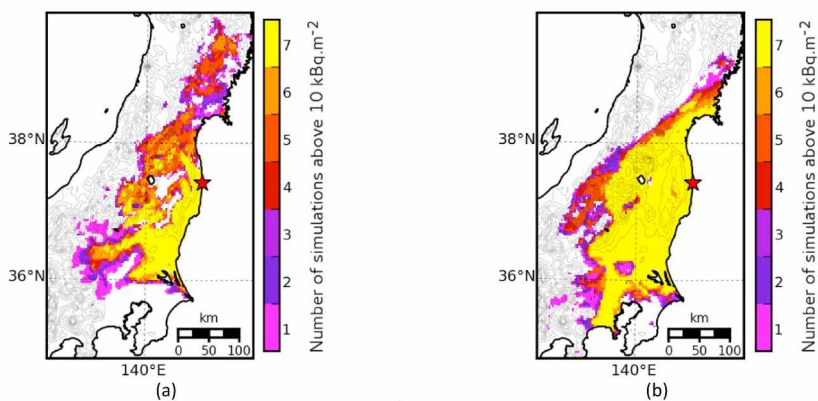
individually, configuration parameters are sometimes influential, but not always, which illustrates the complexity of studying the wet deposition scheme.

5.3. Selecting a wet deposition scheme by comparing with observations

This section uses observed deposit data, as available after the Fukushima accident. To begin with, the three simulations with the highest FMS, FAC2 and PCC scores respectively were selected for a list of

potential candidates for the “best wet deposition scheme”. This scheme must be both effective for all of the statistical indicators, but also reliable in terms of providing an acceptable response, even if an item of input data is incorrectly entered. Secondly, the notion of “best” wet deposition scheme was therefore specified in the context of use for emergency response management.

The three simulations leading to the highest statistical value are identified in Table 7. It appears that these simulations used different meteorological data and source terms. The following wet deposition



Source term	Met. Data	Rain data	Cloud diagnosis	Source term	Met. data	Rain data	Cloud diagnosis
Saunier et al. (2016)	8 th mem. of Sekiyama et al. (2017)	Model	Based on cloud water mixing ratio	Saunier et al. (2013)	1 st mem. of Sekiyama et al. (2017)	Model	Fixed at 500 m

Fig. 8. Zones where the deposits simulated exceed 10 kBq m^{-2} with the seven wet deposition schemes in two configurations. Configurations (a) and (b) are described in the table under their respective figures.

Table 7

Wet deposition scheme used to obtain the highest statistical indicator (FMS, FAC2 and PCC) when compared with deposition observations.

Configuration	Best FMS – 48 %	Best FAC2 – 40 %	Best PCC – 59 %
Wet deposition schemes	<i>NA_wds</i>	<i>ML_wds</i>	<i>NA_wds</i>
Other statistical indicators	FAC2: 35 %; PCC: 55 %	FMS: 48 %; PCC: 43 %	FMS: 43 %; FAC2: 26 %
Source term	Saunier et al. (2016)	Saunier et al. (2013)	Saunier et al. (2016)
Met. Data	8th member of Sekiyama et al. (2017) ensemble	2nd member of Sekiyama et al. (2017) ensemble	1st member of Sekiyama et al. (2017) ensemble
Rain data	Model	Model	Model
Cloud diagnosis	Based on cloud water mixing ratio	Based on cloud water mixing ratio	Based on cloud water mixing ratio

schemes were used: *NA_wds* for FMS and PCC, and *ML_wds* for FAC2. The simulation with the highest FMS obtains relatively good scores for FAC2 (–5% compare to the best FAC2) and PCC, (–4% compare to the best PCC). The simulation with the highest FAC2 also has an FMS equal to the best score. On the other hand, this simulation obtains a very poor PCC score (–16 %). The simulation with the highest PCC has a satisfactory FMS (–5% vs. the highest FMS), but obtains a less satisfactory FAC2

(–14 % vs. the highest score). It would therefore appear that *NA_wds* is the stand-out wet deposition scheme for the best simulation criterion.

However, the wet deposition scheme is intended for use with various types of input data (cf. 2.2) and must ideally lead to results which are as reliable and solid as possible in any context. On this basis, the concept of performance when managing emergency responses led to the definition of several scheme properties: property 1: selecting this scheme (instead of another scheme) generally improves the deposits simulated; property 2: this improvement is significant in this case; property 3: the degradation is never substantial in all other cases.

The impact of selecting one scheme rather than another is estimated based on the difference between the score obtained using this scheme and using another scheme. 216 differences were obtained in this way, from 36 configurations and 6 other schemes used for the purposes of comparison. Fig. 9 shows the distribution of these differences as boxplots with the median value, the first and last quartiles, the first and ninety-nine percentiles and values beyond these percentiles. A median value of 0 % indicates a neutral impact: the statistical indicator is improved (degraded) for half of the simulations using this scheme rather than another scheme. A sub-figure is provided for each statistical indicator.

No scheme has a boxplot entirely above the 0 % horizontal line, which would indicate a systematically preferable scheme. However,

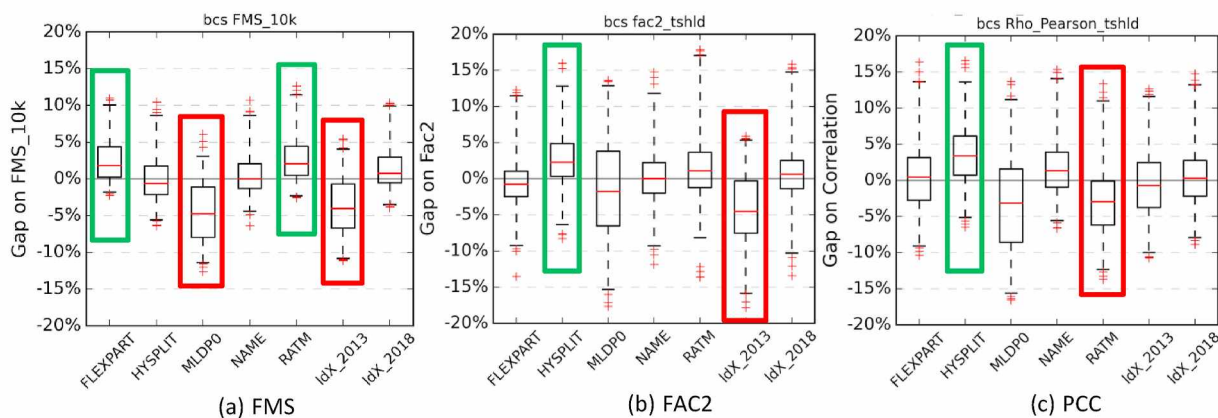


Fig. 9. Comparing the relative impact of wet deposition schemes. Boxplots prepared by comparing simulations with (a) FMS; (b) FAC2; (c) PCC. Green (red) outlines are used for the boxes showing the best (worst) schemes. (For interpretation of the references to colour in this figure legend, the reader is referred to the Web version of this article.)

some boxes are mostly above this line. In best-case conditions, some boxes have the first quartile above the 0 % line, which means that the corresponding scheme improves deposition values in 75 % of cases. At least one scheme satisfies this property for each statistical indicator (framed in green). The reduction in performance is less significant for FMS, negative values do not exceed -13 %, unlike FAC2 and the PCC, where values exceed -15 %. The most insignificant reductions in performance reach 3 % for FMS, 8 % for FAC2 and 7 % for the PCC.

When considering details per scheme, *FL_wds* and *RA_wds* give the best two FMS. *HY_wds* achieves the highest results in terms of FAC2 and PCC, but reduces the FMS (64 % of simulations have less satisfactory results). *RA_wds* gives higher FMS more often (74 % of cases), but reduces the PCC (for 76 % of simulations). *FL_wds* is almost as satisfactory as *RA_wds* in terms of FMS, but is less effective for FAC2 and reduces scores by more than 10 %. *NA_wds* is neutral in terms of FMS and FAC2 scores, while this scheme ranks second in terms of PCC. *ldX_wds2* is the third best scheme for FMS and FAC2, while the PCC remains neutral. Finally, *ML_wds* and *ldX_wds1*, the two schemes with the lowest deposition values, are poorly classified out of the three statistical indicators.

The best FAC2 compared with observations for all of the simulations was obtained with *ML_wds* (cf. Table 8). In this specific configuration, selecting this scheme improves FAC2 compared with the other schemes. However, selecting this scheme is more likely to degrade FAC2 than improve it considering all configurations. On this basis, a scheme can be the best option in the most positive configuration while providing a less efficient performance if several configurations are taken into consideration.

To summarise, according to results, no scheme is systematically more efficient for all three statistical indicators. If no preferable scheme is identified, some schemes will appear as mostly irrelevant considering the inherent systematic errors for some indicators, while other schemes stand out thanks to their more solid impact or at least neutral impact on all indicators.

5.4. Situating a wet deposition scheme by peer comparison

This section focuses on the behaviour of schemes with respect to other schemes. This section considers the different responses suggested by wet deposition schemes independently to observations. Depending on the emergency situation, one specific response may be preferred due to priorities, based on either mean values or by maximising options. In order to reach this decision, preliminary information on the response of a scheme is helpful, particularly to plan for whether the response is likely to be similar to or differ from the other responses. The differences between the responses of schemes were estimated as a mean value for all configurations.

Schemes were compared in pairs for each configuration. The mean value for statistical indicators can be found in Table 8. High mean values are highlighted in blue in this table, for each indicator, while low mean

values are highlighted in yellow. These mean values fall in an interval of between 54 % and 91 % for FMS (Table 8a), between 29 % and 91 % for FAC2 (Table 8b) and between 92 % and 100 % for the PCC (Table 8c). On this basis, the PCC varies little with the wet deposition scheme when compared with FMS or FAC2.

The colour graduation between yellow and blue is almost identical in tables (a) and (b). This infers that FMS and FAC2 identify the same similarities between wet deposition schemes. The two most similar schemes are *ldX_wds2* and *NA_wds* (mean value of FMS and FAC2 = 91 %). Out of all of the other schemes, *HY_wds* is the most similar to *ldX_wds2* and *NA_wds* (with, for example, mean FMS between 84 % and 87 %). *RA_wds* and *FL_wds* are equidistant around this trio, with a mean FMS of 82 % between *FL_wds* and *RA_wds*, and 81 % between *FL_wds* and *ldX_wds2*, for example. The latter two schemes, *ldX_wds1* and *ML_wds* give more dissimilar mean deposits compared to the other five. On this basis, the mean FAC2 between *ML_wds* and *FL_wds* is only 29 %. To summarise, *ldX_wds2*, *NA_wds* and – to a lesser extent, *HY_wds* and *RA_wds* – lead to similar mean results. *FL_wds*, *ML_wds* and *ldX_wds1* give different mean results to the other five simulations.

6. Conclusions and prospects

The performance of an operational atmospheric transport model should constantly be reconsidered in order to optimise responses to future crises. Wet deposition is a key process when predicting soil contamination and therefore for post-accident management. The purpose of this study was to reconsider the role of wet deposition schemes when simulating deposition using an operational model for emergency response management. The case study focuses on the Fukushima accident, which once again raised the question of whether wet deposition models are valid. We carried out a sensitivity study for this purpose, based on the use of several wet deposition schemes and varying the main input parameters used to model wet deposition, in order to integrate some of the complex interactions involved.

According to our results, the wet deposition scheme can have a substantial effect on the simulated deposition map by affecting the distribution of deposits, which highlights the importance of selecting a suitable scheme when managing emergency responses. This impact varies and depends on other modelling parameters: two different schemes can lead to very similar or very different deposition maps for the same event, simply by changing the rest of the configuration (e.g. meteorological data or source term). The modelling of the wet deposition in an operational atmospheric transport model, requires a forewarned choice of the scheme representing it.

The Fukushima accident is still subject to uncertainty due to the complex situation, and wet deposition schemes are applied in simulated conditions which are sometimes not representative of the actual situation. This case study failed to identify a preferable scheme from the list of schemes used in operational models. A further case study, possibly

Table 8

Mean values for statistical indicators for the 21 pairs of wet deposition schemes. The colour code used in the table depends on the value. The schemes are shown in decreasing order of total deposition.

	<i>FL_wds</i>	<i>RA_wds</i>	<i>ldX_wds2</i>	<i>NA_wds</i>	<i>HY_wds</i>	<i>ldX_wds1</i>	<i>ML_wds</i>		<i>FL_wds</i>	<i>RA_wds</i>	<i>ldX_wds2</i>	<i>NA_wds</i>	<i>HY_wds</i>	<i>ldX_wds1</i>	<i>ML_wds</i>		<i>FL_wds</i>	<i>RA_wds</i>	<i>ldX_wds2</i>	<i>NA_wds</i>	<i>HY_wds</i>	<i>ldX_wds1</i>	<i>ML_wds</i>
<i>FL_wds</i>		82%	81%	82%	77%	64%	54%	<i>FL_wds</i>		75%	71%	69%	63%	44%	29%	<i>FL_wds</i>		98%	98%	98%	96%	94%	92%
<i>RA_wds</i>	82%		82%	77%	75%	64%	60%	<i>RA_wds</i>	75%		70%	61%	56%	43%	34%	<i>RA_wds</i>	98%		98%	96%	94%	92%	91%
<i>ldX_wds2</i>	81%	82%		91%	84%	71%	61%	<i>ldX_wds2</i>	71%	70%		91%	77%	52%	32%	<i>ldX_wds2</i>	98%	98%		100%	98%	97%	95%
<i>NA_wds</i>	82%	77%	91%		87%	72%	59%	<i>NA_wds</i>	69%	61%	91%		84%	53%	31%	<i>NA_wds</i>	98%	96%	100%		99%	98%	96%
<i>HY_wds</i>	77%	75%	84%	87%		74%	62%	<i>HY_wds</i>	63%	56%	77%	84%		60%	40%	<i>HY_wds</i>	96%	94%	98%	99%		99%	97%
<i>ldX_wds1</i>	64%	64%	71%	72%	74%		70%	<i>ldX_wds1</i>	44%	43%	52%	53%	60%		58%	<i>ldX_wds1</i>	94%	92%	97%	98%	99%		99%
<i>ML_wds</i>	54%	60%	61%	59%	62%	70%		<i>ML_wds</i>	29%	34%	32%	31%	40%	58%		<i>ML_wds</i>	92%	91%	95%	96%	97%	99%	

based on on-site recordings designed for this purpose, should be investigated in order to improve the modelling of this process.

However, the quality of available data for future crisis management will probably be similar to that of available data for the Fukushima accident. Attempting to identify the best scheme may be fruitless in this context, and efforts must rather be focused on attempting to find better schemes. This study highlights that crisis managers must not exclusively trust a single model for responses. We recommend obtaining both a default scheme, used to provide an initial emergency response, and a panel of schemes, or an envelopes of schemes, with a wide range of known behaviours, allowing an expert to make an informed decision based on the purpose of the evaluation process.

Wet deposition schemes themselves could also be improved. For example, taking into account the electrostatic effects or the particle size diameter like done by von Schonberg et al. (2021).

Declaration of competing interest

The authors declare that they have no known competing financial interests or personal relationships that could have appeared to influence the work reported in this paper.

Acknowledgement

This study was completed as part of the Sakura project, a cooperation programme between the MRI (Japanese Meteorological Research Institute) and the IRSN (French Institute for Radiological Protection and Nuclear Safety). The authors wish to thank Emmanuel Quentric, Alicia Vidal-Allard, Olivier Saunier and Pascal Lemaître for their diligent proofreading of this paper.

References

- AMeDAS, 2011. Automated Meteorological Data Acquisition System.
- Arnold, D., Maurer, C., Wotawa, G., Draxler, R., Saito, K., Seibert, P., 2015. Influence of the meteorological input on the atmospheric transport modelling with FLEXPART of radionuclides from the Fukushima Daiichi nuclear accident. *J. Environ. Radioact.* 139, 212–225. <https://doi.org/10.1016/j.jenvrad.2014.02.013>.
- Champion, D., Korsakissok, I., Didier, D., Mathieu, A., Quélo, D., Groell, J., Quentric, E., Tombette, M., Benoit, J.-P., Saunier, O., Parache, V., Simon-Cornu, M., Gonze, M.A., Renaud, P.H., Cessac, B., Navarro, E., Servant-Perrier, A.-C., 2013. The IRSN's earliest assessments of the Fukushima accident's consequences for the terrestrial environment in Japan. *Radioprotection* 48, 11–37. <https://doi.org/10.1051/radiopro/2012052>.
- Chate, D.M., Pranesha, T.S., 2004. Field studies of scavenging of aerosols by rain events. *J. Aerosol Sci.* 35, 695–706. <https://doi.org/10.1016/j.jaerosci.2003.09.007>.
- Chino, M., Nakayama, H., Nagai, H., Terada, H., Katata, G., Yamazawa, H., 2011. Preliminary estimation of release amounts of ¹³¹I and ¹³⁷Cs accidentally discharged from the Fukushima Daiichi Nuclear Power Plant into the atmosphere. *J. Nucl. Sci. Technol.* 48, 1129–1134. <https://doi.org/10.5194/acpd-11-28319-2011>.
- Costa, M.J., Salgado, R., Santos, D., Levizzani, V., Bortoli, D., Silva, A.M., Pinto, P., 2010. Modelling of orographic precipitation over Iberia: a springtime case study. *Adv. Geosci.* 25, 103–110. <https://doi.org/10.5194/adgeo-25-103-2010>.
- D'Amours, R., Malo, A., 2004. A Zeroth Order Lagrangian Particle Dispersion Model MLDP0.
- Depuydt, G., 2013. Etude expérimentale in-situ du potentiel de lessivage de l'aérosol atmosphérique par les précipitations. Université de Toulouse, St-Paul-lez-Durance.
- Draxler, R., Arnold, D., Chino, M., Galmarini, S., Hort, M., Jones, A., Leadbetter, S., Malo, A., Maurer, C., Rolph, G., Saito, K., Servranckx, R., Shimbori, T., Solazzo, E., Wotawa, G., 2015. World Meteorological Organization's model simulations of the radionuclide dispersion and deposition from the Fukushima Daiichi nuclear power plant accident. *J. Environ. Radioact.* 139, 172–184. <https://doi.org/10.1016/j.jenvrad.2013.09.014>.
- Draxler, R.R., Arnold, D., Galmarini, S., Hort, M.C., Jones, A.R., Leadbetter, S.J., Malo, A., Maurer, C., Rolph, G., Saito, K., Servranckx, R., Shimbori, T., Solazzo, E., Wotawa, G., 2012. Third Meeting of WMO Task Team on Meteorological Analyses for Fukushima-Daiichi Nuclear Power Plant Accident.
- Draxler, R.R., Stunder, B., Rolph, G., Stein, A., Taylor, A., 2016. HYSPLIT User's Guide.
- Duhanyan, N., Roustan, Y., 2011. Below-cloud scavenging by rain of atmospheric gases and particulates. *Atmos. Environ.* 45, 7201–7217. <https://doi.org/10.1016/j.atmosenv.2011.09.002>.
- Eslinger, P.W., Bowyer, T.W., Achim, P., Chai, T., Deconinck, B., Freeman, K., Generoso, S., Hayes, P., Heidmann, V., Hoffman, I., Kijima, Y., Krysta, M., Malo, A., Maurer, C., Ngan, F., Robins, P., Ross, J.O., Saunier, O., Schlosser, C., Schöpner, M., Schrom, B.T., Seibert, P., Stein, A.F., Ungar, K., Yi, J., 2016. International challenge to predict the impact of radionuclides releases from medical isotope production on a comprehensive nuclear test ban treaty sampling station. *J. Environ. Radioact.* 157, 41–51. <https://doi.org/10.1016/j.jenvrad.2016.03.001>.
- Flossmann, A.I., Wobrock, W., 2010. A review of our understanding of the aerosol–cloud interaction from the perspective of a bin resolved cloud scale modelling. *Atmos. Res.* 97, 478–497. <https://doi.org/10.1016/j.atmosres.2010.05.008>.
- Girard, S., Mallet, V., Korsakissok, I., Mathieu, A., 2016. Emulation and Sobol' sensitivity analysis of an atmospheric dispersion model applied to the Fukushima nuclear accident. *J. Geophys. Res. Atmos.* 121, 3484–3496. <https://doi.org/10.1002/2015jd023993>.
- Groell, J., Quélo, D., Mathieu, A., 2014. Sensitivity analysis of the modelled deposition of ¹³⁷Cs on the Japanese land following the Fukushima accident. *Int. J. Environ. Pollut.* 55, 67–75. <https://doi.org/10.1504/ijep.2014.065906>.
- Hertel, O., Christensen, J.H., Runge, E.H., Asman, W.A.H., Berkowicz, R., Hovmand Mads, F., 1995. Development and testing of a new variable scale air pollution model - ACDEP. *Atmos. Environ.* 29, 1267–1290. [https://doi.org/10.1016/1352-2310\(95\)00067-9](https://doi.org/10.1016/1352-2310(95)00067-9).
- Hirose, K., 2016. Fukushima Daiichi Nuclear Plant accident: atmospheric and oceanic impacts over the five years. *J. Environ. Radioact.* 157, 113–130. <https://doi.org/10.1016/j.jenvrad.2016.01.011>.
- Hososhima, M., Kaneyasu, N., 2015. Altitude-dependent distribution of ambient gamma dose rates in a mountainous area of Japan caused by the Fukushima nuclear accident. *Environ. Sci. Technol.* 49, 3341–3348. <https://doi.org/10.1021/es504838w>.
- Kajino, M., Sekiyama, T.T., Igarashi, Y., Katata, G., Sawada, M., Adachi, K., Zaizen, Y., Tsuruta, H., Nakajima, T., 2019. Deposition and dispersion of radio-cesium released due to the Fukushima nuclear accident: sensitivity to meteorological models and physical modules. *J. Geophys. Res. Atmos.* <https://doi.org/10.1029/2018JD028998>.
- Katata, G., Chino, M., Kobayashi, T., Terada, H., Ota, M., Nagai, H., Kajino, M., Draxler, R., Hort, M.C., Malo, A., Torii, T., Sanada, Y., 2015. Detailed source term estimation of the atmospheric release for the Fukushima Daiichi Nuclear Power Station accident by coupling simulations of atmospheric dispersion model with improved deposition scheme and oceanic dispersion model. *Atmos. Chem. Phys.* 15, 1029–1070. <https://doi.org/10.5194/acp-15-1029-2015>.
- Kerker, M., Hampl, V., 1974. Scavenging of aerosol particles by a falling water drops and quality of washout coefficients. *J. Atmos. Sci.* 31, 1368–1376.
- Kitayama, K., Morino, Y., Takigawa, M., Nakajima, T., Hayami, H., Nagai, H., Terada, H., Saito, K., Shimbori, T., Kajino, M., Sekiyama, T.T., Didier, D., Mathieu, A., Quélo, D., Ohara, T., Tsuruta, H., Oura, Y., Ebihara, M., Moriguchi, Y., Shibata, T., 2018. Atmospheric modeling of ¹³⁷Cs plumes from the Fukushima Daiichi nuclear power plant-evaluation of the model intercomparison data of the science Council of Japan. *J. Geophys. Res. Atmos.* <https://doi.org/10.1029/2017JD028230>.
- Korsakissok, I., Mathieu, A., Didier, D., 2013. Atmospheric dispersion and ground deposition induced by the Fukushima Nuclear power plant accident : a local scale simulation and sensitivity study. *Atmos. Environ.* 70, 267–279. <https://doi.org/10.1016/j.atmosenv.2013.01.002>.
- Laakso, L., Grönholm, T., Rannik, Ü., Kosmale, M., Fiedler, V., Vehkamäki, H., Kulmala, M., 2003. Ultrafine particle scavenging coefficients calculated from 6 years field measurements. *Atmos. Environ.* 37, 3605–3613. [https://doi.org/10.1016/S1352-2310\(03\)00326-1](https://doi.org/10.1016/S1352-2310(03)00326-1).
- Lai, K.-Y., Dayan, N., Kerker, M., 1978. Scavenging of aerosol particles by a falling water drop. *J. Atmos. Sci.* 35, 674–682.
- Leadbetter, S.J., 2019. Use of radar rainfall to model deposition of radionuclides. *Atmos. Environ.* [S1352231019302833. https://doi.org/10.1016/j.atmosenv.2019.04.056](https://doi.org/10.1016/j.atmosenv.2019.04.056).
- Leadbetter, S.J., Hort, M.C., Jones, A.R., Webster, H.N., Draxler, R.R., 2015. Sensitivity of the modelled deposition of Caesium-137 from the Fukushima Dai-ichi nuclear power plant to the wet deposition parameterisation in NAME. *J. Environ. Radioact.* 139, 200–211. <https://doi.org/10.1016/j.jenvrad.2014.03.018>.
- Lemaître, P., Quérel, A., Monier, M., Menard, T., Porcheron, E., Flossmann, A.I., 2017. Experimental evidence of the rear capture of aerosol particles by raindrops. *Atmos. Chem. Phys.* 17, 4159–4176. <https://doi.org/10.5194/acp-17-4159-2017>.
- Louis, J.-F., Tiedtke, M., Geleyn, J.F., 1981. A Short History of the Operational PBL - Parameterization at ECMWF. Presented at the ECMWF Workshop on PBL Parameterization, Reading, U.K., pp. 59–79.
- Makhon'ko, K.P., 1967. Simplified theoretical notion of contaminant removal by precipitation from the atmosphere. *Tellus* 19, 467–476. <https://doi.org/10.3402/tellusa.v19i3.9815>.
- Mallet, V., Quélo, D., Sportisse, B., Ahmed de Biasi, M., Debry, é., Korsakissok, I., Wu, L., Roustan, Y., Sartelet, K., Tombette, M., Foudhil, H., 2007. Technical Note: the air quality modeling system Polyphemus. *Atmos. Chem. Phys.* 7, 5479–5487. <https://doi.org/10.5194/acp-7-5479-2007>.
- Mallet, V., Sportisse, B., 2004. 3-D chemistry-transport model Polair: numerical issues, validation and automatic-differentiation strategy. *Atmos. Chem. Phys. Discuss.* 4, 1371–1392.
- Marzo, G.A., 2014. Atmospheric transport and deposition of radionuclides released after the Fukushima Dai-ichi accident and resulting effective dose. *Atmos. Environ.* 94, 709–722. <https://doi.org/10.1016/j.atmosenv.2014.06.009>.
- Mathieu, A., Kajino, M., Korsakissok, I., Périllat, R., Quélo, D., Quérel, A., Saunier, O., Sekiyama, T.T., Igarashi, Y., Didier, D., 2018. Fukushima Daiichi-derived radionuclides in the atmosphere, transport and deposition in Japan: a review. *Appl. Geochem.* 91, 122–139. <https://doi.org/10.1016/j.apgeochem.2018.01.002>.
- Mathieu, A., Korsakissok, I., Quélo, D., Groell, J., Tombette, M., Didier, D., Quentric, E., Saunier, O., Benoit, J.-P., 2012. Assessment of atmospheric dispersion for the Fukushima Dai-ichi nuclear power plant accident. In: Presented at the 13th International Congress of the International Radiation Protection Association.
- Maurer, C., Baré, J., Kusmierczyk-Michulec, J., Crawford, A., Eslinger, P.W., Seibert, P., Orr, B., Philipp, A., Ross, O., Generoso, S., Achim, P., Schoeppner, M., Malo, A.,

- Ringbom, A., Saunier, O., Quérel, D., Mathieu, A., Kijima, Y., Stein, A., Chai, T., Ngan, F., Leadbetter, S.J., De Meutter, P., Delcloo, A., Britton, R., Davies, A., Glascoe, L.G., Lucas, D.D., Simpson, M.D., Vogt, P., Kalinowski, M., Bowyer, T.W., 2018. International challenge to model the long-range transport of radionuclides released from medical isotope production to six Comprehensive Nuclear-Test-Ban Treaty monitoring stations. *J. Environ. Radioact.* 192, 667–686. <https://doi.org/10.1016/j.jenvrad.2018.01.030>.
- MEXT, 2011a. Results of the Fourth Airborne Monitoring Survey by MEXT.
- MEXT, 2011b. Reading of Environmental Radioactivity Level by Prefecture (Fallout) [WWW Document]. *Environ. Monit. Data - Jpn. At. Energy Agency*. <http://emdb.jaea.go.jp/emdb/en/portals/50100000001/>.
- Morino, Y., Ohara, T., Nishizawa, M., 2011. Atmospheric behavior, deposition, and budget of radioactive materials from the Fukushima Daiichi nuclear power plant in March 2011. *Geophys. Res. Lett.* 38, L00G11 <https://doi.org/10.1029/2011gl048689>.
- Morino, Y., Ohara, T., Watanabe, M., Hayashi, S., Nishizawa, M., 2013. Episode analysis of deposition of radiocesium from the Fukushima Daiichi nuclear power plant accident. *Environ. Sci. Technol.* 47, 2314–2322. <https://doi.org/10.1021/es304620x>.
- MRI, 2015. JMA-RATM Technical Report, vol. 76. E.
- Nakajima, T., Misawa, S., Morino, Y., Tsuruta, H., Goto, D., Uchida, J., Takemura, T., Ohara, T., Oura, Y., Ebihara, M., Satoh, M., 2017. Model depiction of the atmospheric flows of radioactive cesium emitted from the Fukushima Daiichi Nuclear Power Station accident. *Prog. Earth Planet. Sci.* 4, 18. <https://doi.org/10.1186/s40645-017-0117-x>.
- Oura, Y., Ebihara, M., Tsuruta, H., Nakajima, T., Ohara, T., Ishimoto, M., Sawahata, H., Nitta, W., 2015. A database of hourly atmospheric concentrations of radiocesium (134Cs and 137Cs) in suspended particulate matter collected in March 2011 at 99 air pollution monitoring stations in Eastern Japan. *J. Nucl. Radiochem. Sci.* 15, 1–12.
- Pudykiewicz, J., 1989. Simulation of the Chernobyl dispersion with a 3-D hemispheric tracer model. *Tellus* 41B, 391–412.
- Quérel, D., Krysta, M., Bocquet, M., Isnard, O., Minier, Y., Sportisse, B., 2007. Validation of the Polyphemus platform on the ETEX, Chernobyl and algeiras cases. *Atmos. Environ.* 41, 5300–5315. <https://doi.org/10.1016/j.atmosenv.2007.02.035>.
- Quérel, A., 2017. Cloud Diagnosis Impact on Deposition Modelling Applied to the Fukushima Accident.
- Quérel, A., Lemaître, P., Monier, M., Porcheron, E., Flossmann, A.I., Hervo, M., 2014a. An experiment to measure raindrop collection efficiencies: influence of rear capture. *Atmos. Meas. Tech.* 7, 1321–1330. <https://doi.org/10.5194/amt-7-1321-2014>.
- Quérel, A., Monier, M., Flossmann, A.I., Lemaître, P., Porcheron, E., 2014b. The importance of new collection efficiency values including the effect of rear capture for the below-cloud scavenging of aerosol particles. *Atmos. Res.* 142, 57–66. <https://doi.org/10.1016/j.atmosres.2013.06.008>.
- Quérel, A., Quérel, D., Roustan, Y., Mathieu, A., Kajino, M., Sekiyama, T., Adachi, K., Didier, D., Igarashi, Y., Maki, T., 2016. Fukushima: Lessons Learned on Wet Deposition from a Combined Analysis of Radiation Dose Rate and Volume Activity Measurements of 137Cesium. Presented at the Goldschmidt Conference, Yokohama, p. 2561.
- Quérel, A., Roustan, Y., Quérel, D., Benoit, J.-P., 2015. Hints to discriminate the choice of wet deposition models applied to an accidental radioactive release. *Int. J. Environ. Pollut.* 58, 268–279. <https://doi.org/10.1504/IJEP.2015.077457>.
- Saito, K., Shimbori, T., Draxler, R., 2015. JMA's regional atmospheric transport model calculations for the WMO technical task team on meteorological analyses for Fukushima Daiichi Nuclear Power Plant accident. *J. Environ. Radioact.* 139, 185–199. <https://doi.org/10.1016/j.jenvrad.2014.02.007>.
- Sanada, Y., Katata, G., Kaneyasu, N., Nakanishi, C., Urabe, Y., Nishizawa, Y., 2018. Altitudinal characteristics of atmospheric deposition of aerosols in mountainous regions: Lessons from the Fukushima Daiichi Nuclear Power Station accident. *Sci. Total Environ.* 618, 881–890. <https://doi.org/10.1016/j.scitotenv.2017.08.246>.
- Sato, Y., Sekiyama, T.T., Fang, S., Kajino, M., Quérel, A., Quérel, D., Kondo, H., Terada, H., Kadowaki, M., Takigawa, M., Morino, Y., Uchida, J., Goto, D., Yamazawa, H., 2020. A model intercomparison of atmospheric 137Cs concentrations from the Fukushima Daiichi Nuclear Power Plant accident, phase III: simulation with an identical source term and meteorological field at 1-km resolution. *Atmos. Environ.* X 7, 100086. <https://doi.org/10.1016/j.aeaoa.2020.100086>.
- Sato, Y., Takigawa, M., Sekiyama, T.T., Kajino, M., Terada, H., Nagai, H., Kondo, H., Uchida, J., Goto, D., Quérel, D., Mathieu, A., Quérel, A., Fang, S., Morino, Y., von Schoenberg, P., Grahm, H., Brännström, N., Hirao, S., Tsuruta, H., Yamazawa, H., Nakajima, T., 2018. Model intercomparison of atmospheric ¹³⁷Cs from the Fukushima Daiichi Nuclear Power Plant accident: simulations based on identical input data. *J. Geophys. Res. Atmos.* <https://doi.org/10.1029/2018JD029144>.
- Saunier, O., Didier, D., Mathieu, A., Korsakissok, I., 2019. Real-time use of inverse modeling techniques to assess the atmospheric accidental release of a nuclear power plant. In: Proceedings of the 5th NERIS Workshop. Presented at the NERIS Workshop 2019, Roskilde, Denmark.
- Saunier, O., Mathieu, A., Didier, D., Tombette, M., Quérel, D., Winiarek, V., Bocquet, M., 2013. An inverse modelling method to assess the source term of the Fukushima Nuclear Power Plant accident using gamma dose rate observations. *Atmos. Chem. Phys.* 13, 11403–11421. <https://doi.org/10.5194/acp-13-11403-2013>.
- Saunier, O., Mathieu, A., Sekiyama, T.T., Kajino, M., Adachi, K., Bocquet, M., Maki, T., Higarashi Didier, D., 2016. A New Perspective on the Fukushima Releases Brought by Newly Available 137Cs Air Concentration Observations and Reliable Meteorological Fields. Presented at the 17th International Conference on Harmonisation within Atmospheric Dispersion Modelling for Regulatory Purposes. Budapest, Hungary.
- Science Council of Japan SCJ, 2014. A Review of the Model Comparison of Transportation and Deposition of Radioactive Materials Released to the Environment as a Result of the Tokyo Electric Power Company's Fukushima Daiichi Nuclear Power Plant Accident, Committee on Comprehensive Synthetic Engineering. Science Council of Japan. Science Council of Japan.
- Sekiyama, T.T., Kajino, M., Kunii, M., 2017. The impact of surface wind data assimilation on the predictability of near-surface plume advection in the case of the Fukushima nuclear accident. *J. Meteorol. Soc. Jpn. Ser. II* 95, 447–454. <https://doi.org/10.2151/jmsj.2017-025>.
- Sekiyama Thomas, Tsuyoshi, Kajino, Mizuo, Kunii, Masaru, et al., 2021. Ensemble dispersion simulation of a point-source radioactive aerosol using perturbed meteorological fields over eastern Japan. *Atmosphere* 12 (6), 662. <https://doi.org/10.3390/atmos12060662>.
- Slinn, W.G.N., 1977. Some approximations for the wet and dry removal of particles and gases from the atmosphere. *Water, Air, Soil Pollut.* 7, 513–543.
- Stephan, K., Klink, S., Schraff, C., 2008. Assimilation of radar-derived rain rates into the convective-scale model COSMO-DE at DWD. *Q. J. R. Meteorol. Soc.* 134, 1315–1326. <https://doi.org/10.1002/qj.269>.
- Terada, H., Katata, G., Chino, M., Nagai, H., 2012. Atmospheric discharge and dispersion of radionuclides during the Fukushima Dai-ichi Nuclear Power Plant accident. Part II: verification of the source term and analysis of regional-scale atmospheric dispersion. *J. Environ. Radioact.* 112, 141–154. <https://doi.org/10.1016/j.envrad.2012.05.023>.
- Terasaka, Y., Yamazawa, H., Jun, H., Shigekazu, H., Hiroki, S., Jun, M., Yu, K., 2016. Air concentration estimation of radionuclides discharged from Fukushima Daiichi Nuclear Power Station using NaI(Tl) detector pulse height distribution measured in Ibaraki Prefecture. *J. Nucl. Sci. Technol.* 1–14. <https://doi.org/10.1080/00223131.2016.1193453>.
- Troen, I., Mahrt, L., 1986. A simple model of atmospheric boundary layer; sensitivity to surface evaporation. *Bound. Layer Meteorol.* 37, 129–148.
- Tsuruta, H., Oura, Y., Ebihara, M., Ohara, T., Nakajima, T., 2014. First retrieval of hourly atmospheric radionuclides just after the Fukushima accident by analyzing filter-tapes of operational air pollution monitoring stations. *Sci. Rep.* 4, 1–10. <https://doi.org/10.1038/srep06717>.
- Volken, M., Schumann, T., 1993. A critical review of below-cloud aerosol scavenging results on Mt Rigi. *Water, Air, Soil Pollut.* 68, 15–28.
- Wang, X., Zhang, L., Moran, M.D., 2011. On the discrepancies between theoretical and measured below-cloud particle scavenging coefficients for rain – a numerical investigation using a detailed one-dimensional cloud microphysics model. *Atmos. Chem. Phys.* 11, 11859–11866. <https://doi.org/10.5194/acp-11-11859-2011>.
- Yumimoto, K., Morino, Y., Ohara, T., Oura, Y., Ebihara, M., Tsuruta, H., Nakajima, T., 2016. Inverse modeling of the 137Cs source term of the Fukushima Dai-ichi Nuclear Power Plant accident constrained by a deposition map monitored by aircraft. *J. Environ. Radioact.* 164, 1–12. <https://doi.org/10.1016/j.jenvrad.2016.06.018>.
- Zhang, L., Gong, S., Padro, J., Barrie, L., 2001. A size-segregated particle dry deposition scheme for an atmospheric aerosol module. *Atmos. Environ.* 35, 549–560. [https://doi.org/10.1016/S1352-2310\(00\)00326-5](https://doi.org/10.1016/S1352-2310(00)00326-5).
- Zhang, L., Wang, X., Moran, M.D., Feng, J.Q., 2013. Review and uncertainty assessment of size-resolved scavenging coefficient formulations for below-cloud snow scavenging of atmospheric aerosols. *Atmos. Chem. Phys.* 13, 10005–10025.